Renewable Energy 50 (2013) 161–167

Contents lists available at SciVerse ScienceDirect

Renewable Energy

journal homepage: www.elsevier.com/locate/renene

Ray tracing and simulation for the beam-down solar concentrator

Xiudong Wei*, Zhenwu Lu, Weixing Yu, Wenbin Xu

Changchun Institute of Optics, Fine Mechanics and Physics, Chinese Academy of Sciences, Changchun, 130033, China

ARTICLE INFO

Article history:
Received 9 August 2011
Accepted 18 June 2012
Available online 20 July 2012

Keywords:
Beam-down solar concentrator
Heliostat
Tower reflector
CPC
Ray tracing

ABSTRACT

The ray tracing equations for the beam-down solar concentrator have been derived in this paper. Based on the equations, a new module for the simulation of the beam-down solar concentrating system has been developed and incorporated into the code HFLD. To validate the ray tracing equations, a simple beam-down solar concentrating system consisting of 3 heliostats and a hyperboloid reflector is simulated. The concentrated spots at the lower focal point of the hyperboloid reflector for the beam-down system are calculated by the modified code HFLD and then compared with that calculated by the commercial software Zemax. It is found that the calculated results coincide with each other basically. Furthermore, a beam-down solar concentrator consisting of 31 heliostats, a tower reflector and a CPC is designed and simulated by using the modified code HFLD. The concentrated spots of the beam-down solar concentrator are calculated.

1. Introduction

For the solar tower system, the tower is designed to be very high in order to reduce the losses including the cosine loss, the shading loss and the blocking loss and so on [1]. However, to place the heavy receiver atop the very high tower will result in a rather high tower cost. In addition, the working fluid needs to be pumped up to the top of the tower so that the exceptional power is consumed. Finally, the heat loss is also very high when the heat transfers from the receiver to the energy converter. To overcome above mentioned shortcomings, the beam-down solar concentrator has been proposed and developed. The beam-down concept was firstly proposed by Rabl [2], and further investigated by Segal et al. [3–6], Kribus et al. [7], Hasuike et al. [8] and Wieckert et al. [9]. An operational beam-down solar system has been constructed at the Weizmann-Institute. According to Segal et al. [4], the tower reflector with a hyperboloid surface is suitable for the beam-down concentrator. However, the hyperboloid reflector always magnifies the sun image and thus results in a lower concentration factor. Therefore, a second concentrator, i.e. the receiver concentrator (RC), is necessary to improve the concentration factor. The CPC (compound parabolic concentrator) is usually selected as the RC in that it approaches the ideal case and therefore has the maximum concentration factor in theory. In the design of the beam-down concentrator, the performance of the concentrator at any time over a year should be evaluated and analyzed. However, this is almost impossible by using the existing commercial software because of the awkward inputs and complex calculations. Therefore, it is necessary to derive the ray tracing equations and then based on which to develop a simulation module for the beam-down solar concentrator.

In this work, the ray tracing equations for the beam-down solar concentrator have been derived. Based on the ray tracing equations, a new module has been developed and incorporated into the code HFLD [10,11]. The correctness of the ray tracing equations is proved by comparing the concentrated spots at the lower focal point of the hyperboloid reflector calculated by both the modified code HFLD and the commercial software Zemax. Finally, a beam-down solar concentrator consisting of 31 heliostats, a tower reflector and a CPC is designed and simulated by using the modified code HFLD. The concentrated spot of the designed beam-down concentrator at different time over a year is calculated. This work is helpful for the design of the beam-down concentrator in the solar thermal applications. The derivation and validation of the ray-tracing equations for the beam-down concentrator is worthwhile for the community.

2. Ray tracing equations

The beam-down solar concentrator consists of a heliostat field, a tower reflector and a receiver concentrator and is shown in Fig. 1. The heliostats track the sun and reflect the sunlight to the aim point T. The tower reflector redirects the concentrated solar radiation down onto the RC entrance located at near the ground level. The heliostats can be flat or curved. The shape of the tower reflector is

* Corresponding author. Fax: +86431 8617 6295.
E-mail address: wei.xiudong@yahoo.com.cn (X. Wei).

0960-1481/$ – see front matter © 2012 Elsevier Ltd. All rights reserved.
http://dx.doi.org/10.1016/j.renene.2012.06.029

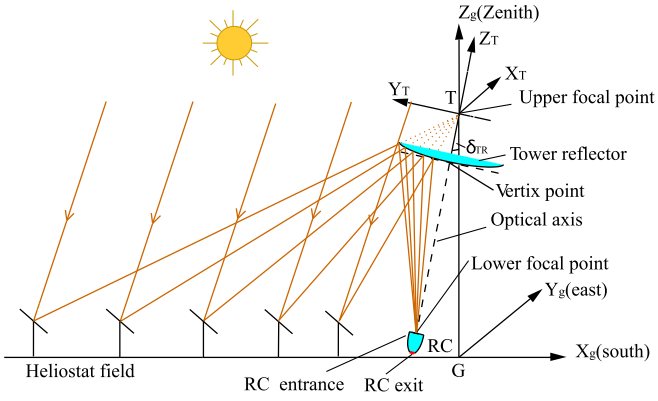

Fig. 1. Schematic of the beam-down solar concentrator and coordinate systems.

usually a hyperboloid which has two focal points: upper focal point and lower focal point. The aim point T coincides with the upper focal point of the tower reflector. The optical axis coincides with the symmetric axis of the hyperboloid. The lower focal point of the hyperboloid is located on the RC entrance plane. The solar image at the lower focal point is magnified by the ratio: $(L - z_0)/z_0$, where L is the distance between the lower focal point and the aim point T and z_0 is the distance between the vertex point of the tower reflector and the aim point T. The magnification also depends on the shape of the tower reflector. Furthermore, the shape of the tower reflector depends on L and z_0. The RC concentrates the radiation again onto the receiver so that a required concentration factor can be obtained finally. For modeling and designing the beam-down solar concentrator, it is necessary to derive the ray tracing equations. To do this, Cartesian right-handed coordinate systems are established and illustrated in Fig. 1. Ground-coordinate axes are defined as X_g, Y_g, Z_g, where the tower base center G is the origin, X_g axis points toward south, Y_g axis points toward east, and Z_g axis points toward the zenith. Target coordinate axes are defined as X_T, Y_T, Z_T, where the aim point T is the origin, Z_T axis is along the optical axis direction of the tower reflector surface and in the plane defined by Z_g axis and X_g axis, X_T axis is parallel to Y_g axis and points toward east, Y_T axis is perpendicular to X_T axis and Z_T axis, X_T and Y_T are located in the aim plane. δ_{TR} is the tilt angle of the tower reflector which equals to the angle between Z_T axis and Z_g axis.

The equations of the traced ray between the heliostat and the tower reflector in the target coordinates is written as follows,

$$\frac{x - x_T}{\cos\alpha_t} = \frac{y - y_T}{\cos\beta_t} = \frac{z}{\cos\gamma_t} \tag{1}$$

where (x_T, y_T) are the coordinates of intersection point between the traced ray and the aim plane, and $(\cos\alpha_t, \cos\beta_t, \cos\gamma_t)$ are the direction cosine components of the traced ray in the target coordinate axes. The derivation for the Eq. (1) was presented in our previous paper (Wei et al. 2007).

The tower reflector must have the property to reflect all rays concentrated to a point, the aim point, so that they pass through the same final point, the image point. A surface with these characteristics is called a Cartesian surface. The surface equation of the tower reflector in the form $z = f(x,y)$ is given as follows [12],

$$z = f(x,y) = \frac{(x^2 + y^2)/R}{1 + \left[1 - (1+k)\cdot(x^2 + y^2)/R^2\right]^{1/2}} \tag{2}$$

where R is the vertex curvature radius of the surface, and k is the conic constant. If $k < -1$, Eq. (2) represents a hyperboloid surface of two sheets.

The direction cosine components $(\cos\alpha_{n1}, \cos\beta_{n1}, \cos\gamma_{n1})$ of the normal vector at a point of the tower reflector surface in the target coordinate axes are written as follows,

$$(\cos\alpha_{n1}, \cos\beta_{n1}, \cos\gamma_{n1}) = \left(f_x, f_y, 1\right) \Big/ \left(f_x^2 + f_y^2 + 1\right)^{1/2} \tag{3}$$

where f_x, f_y denote the partial derivatives of Eq. (2) for x and y.

By inserting Eq. (1) into Eq. (2) and solving x, y and z, the coordinates (x_1, y_1, z_1) of the intersection point between the traced ray and the tower reflector surface can be obtained. Then, by inserting (x_1, y_1, z_1) into Eq. (3), the normal vector at intersection point of the tower reflector surface can be obtained.

According to the Snell law, the direction cosine components $(\cos\alpha_{r1}, \cos\beta_{r1}, \cos\gamma_{r1})$ of the reflection ray on the tower reflector surface in the target coordinate axes are written as follows,

$$\begin{bmatrix} \cos\alpha_{r1} \\ \cos\beta_{r1} \\ \cos\gamma_{r1} \end{bmatrix} = \begin{bmatrix} 2\cdot\cos\theta_1\cdot\cos\alpha_{n1} - \cos\alpha_t \\ 2\cdot\cos\theta_1\cdot\cos\beta_{n1} - \cos\beta_t \\ 2\cdot\cos\theta_1\cdot\cos\gamma_{n1} - \cos\gamma_t \end{bmatrix} \tag{4}$$

where θ_1 is the reflection angle and the cosine of θ_1 can be written as,

$$\cos\theta_1 = \cos\alpha_t\cdot\cos\alpha_{n1} + \cos\beta_t\cdot\cos\beta_{n1} + \cos\gamma_t\cdot\cos\gamma_{n1} \tag{5}$$

In terms of the target coordinate axes, the equations of the reflection ray on the tower reflector are written as follows,

$$\frac{x - x_1}{\cos\alpha_{r1}} = \frac{y - y_1}{\cos\beta_{r1}} = \frac{z - z_1}{\cos\gamma_{r1}} \tag{6}$$

In Fig. 2, RC coordinate axes are defined as X_{RC}, Y_{RC}, Z_{RC}, where the RC entrance aperture center is the origin, Z_{RC} axis is along the normal direction of the RC aperture plane and located in the plane defined by Z_g axis and X_g axis, X_{RC} axis is parallel to the Y_g axis and points toward east, Y_{RC} axis is perpendicular to X_{RC} axis and Z_{RC} axis. X_{RC} axis and Y_{RC} axis are located in the entrance aperture plane. L is the distance between the aim point T and the RC entrance aperture center. δ_{RC} is the tilt angle of the entrance aperture plane which equals to the angle between Z_{RC} axis and Z_T axis.

Using Eq. (6), the coordinates (X_r, Y_r, Z_r) of intersection point between the traced ray and the plane $Z_T = -L$ (see Fig. 2) can be solved as follows,

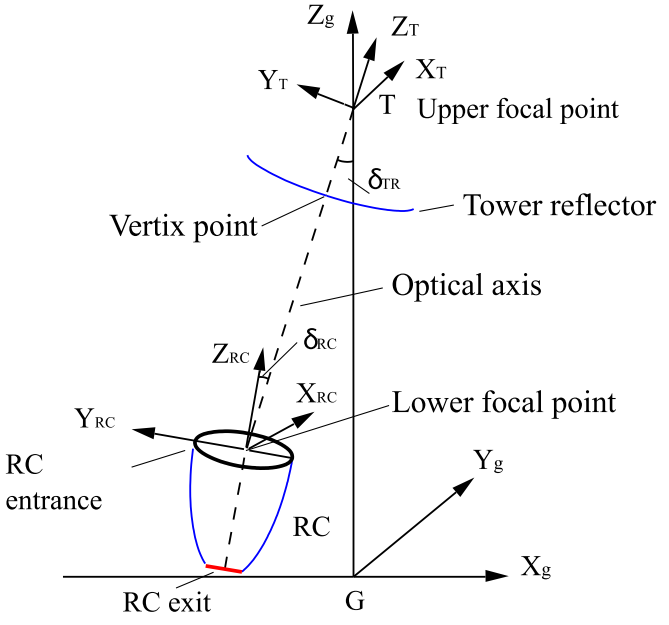

Fig. 2. Schematic of the RC and coordinate axes.

Table 1
Parameters of the heliostats and tower reflector.

Heliostat size	2.1 m × 2.1 m
Height of heliostat h_h	1.2 m
Coordinates of the heliostats (x_g,y_g)	(−13.44,0), (−20.71,0), (−29.43,0)
Aim point height h_A	12 m
Latitude Φ	40.4°
Surface shape of heliostat	Spherical
Tracking method of heliostat	Azimuth-elevation tracking
Tower reflector size	2.5 m × 4.5 m
Vertex curvature radius R	16.195 m
Conic constant δ	−2.729
Height of tower reflector h_T	10.17 m
Tilt angle of tower reflector δ_{TR}	33.4°

$$\begin{bmatrix} X_r \\ Y_r \\ Z_r \end{bmatrix} = \begin{bmatrix} (-L-z_1)\cdot\cos\alpha_{r1}/\cos\gamma_{r1}+x_1 \\ (-L-z_1)\cdot\cos\beta_{r1}/\cos\gamma_{r1}+y_1 \\ -L \end{bmatrix} \tag{7}$$

A new auxiliary coordinate axis is obtained by translating the target coordinate axes for $-L$ along Z_T axis. In terms of the new coordinate axes, the coordinates of the intersection point between the traced ray and the plane $Z_T = -L$ can be written as $(X_r, Y_r, 0)$, which can then be transformed from the new auxiliary coordinate axes to RC coordinate axes by using the transformation matrix M. M is given as follows,

$$M = \begin{bmatrix} 1 & 0 & 0 \\ 0 & \cos\delta_{RC} & -\sin\delta_{RC} \\ 0 & \sin\delta_{RC} & \cos\delta_{RC} \end{bmatrix} \tag{8}$$

Thus we have,

$$\begin{bmatrix} X_{\mathrm{rc}} \\ Y_{\mathrm{rc}} \\ Z_{\mathrm{rc}} \end{bmatrix} = \begin{bmatrix} X_r \\ Y_r\cdot\cos\delta_{RC} \\ Y_r\cdot\sin\delta_{RC} \end{bmatrix} \tag{9}$$

And,

$$\begin{bmatrix} \cos\alpha_{\mathrm{rc}} \\ \cos\beta_{\mathrm{rc}} \\ \cos\gamma_{\mathrm{rc}} \end{bmatrix} = \begin{bmatrix} \cos\alpha_r \\ \cos\beta_r\cdot\cos\delta_{\mathrm{RC}}-\cos\gamma_r\cdot\sin\delta_{\mathrm{RC}} \\ \cos\beta_r\cdot\sin\delta_{\mathrm{RC}}+\cos\gamma_r\cdot\cos\delta_{\mathrm{RC}} \end{bmatrix} \tag{10}$$

where (X_{rc}, Y_{rc}, Z_{rc}) denote the coordinates of intersection point between the traced ray and the RC entrance aperture plane, $(\cos\alpha_{rc}, \cos\beta_{rc}, \cos\gamma_{rc})$ denote the direction cosine components of the traced ray in the RC coordinate axes.

The coordinates (X_A, Y_A, Z_A) of the intersection point between the traced ray and the RC entrance aperture plane are derived as follows,

$$\begin{bmatrix} x_A \\ y_A \\ z_A \end{bmatrix} = \begin{bmatrix} -Z_{\mathrm{rc}}\cdot\cos\alpha_{rc}/\cos\gamma_{rc}+X_{rc} \\ -Z_{\mathrm{rc}}\cdot\cos\beta_{rc}/\cos\gamma_{rc}+Y_{rc} \\ 0 \end{bmatrix} \tag{11}$$

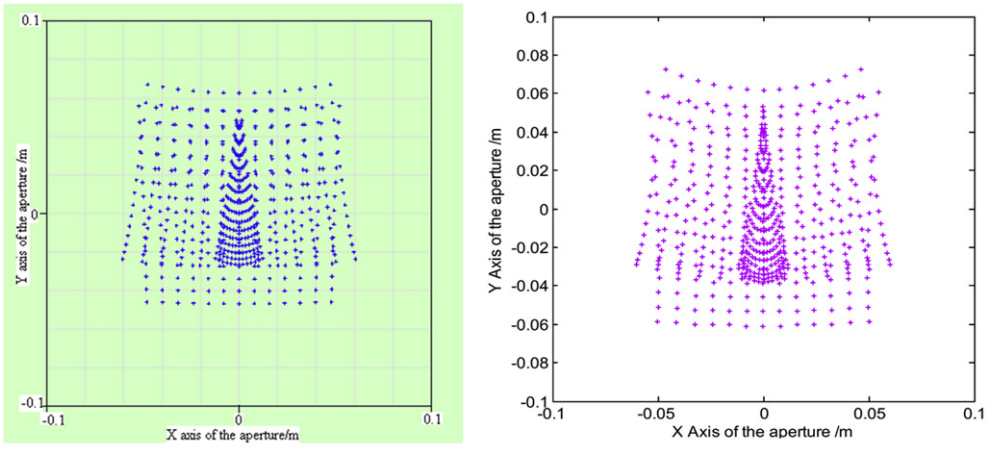

a At noon on vernal equinox

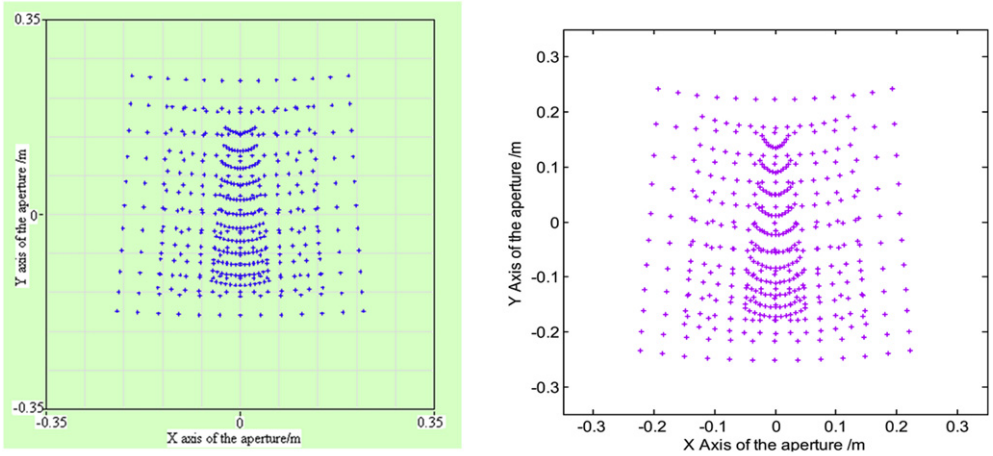

b At noon on summer solstice

Fig. 3. A comparison of concentrated spots at the lower focal point of the tower reflector for the beam-down system calculated by Zemax (left side) and modified code HFLD (right side), the dimensions shown are in meters.

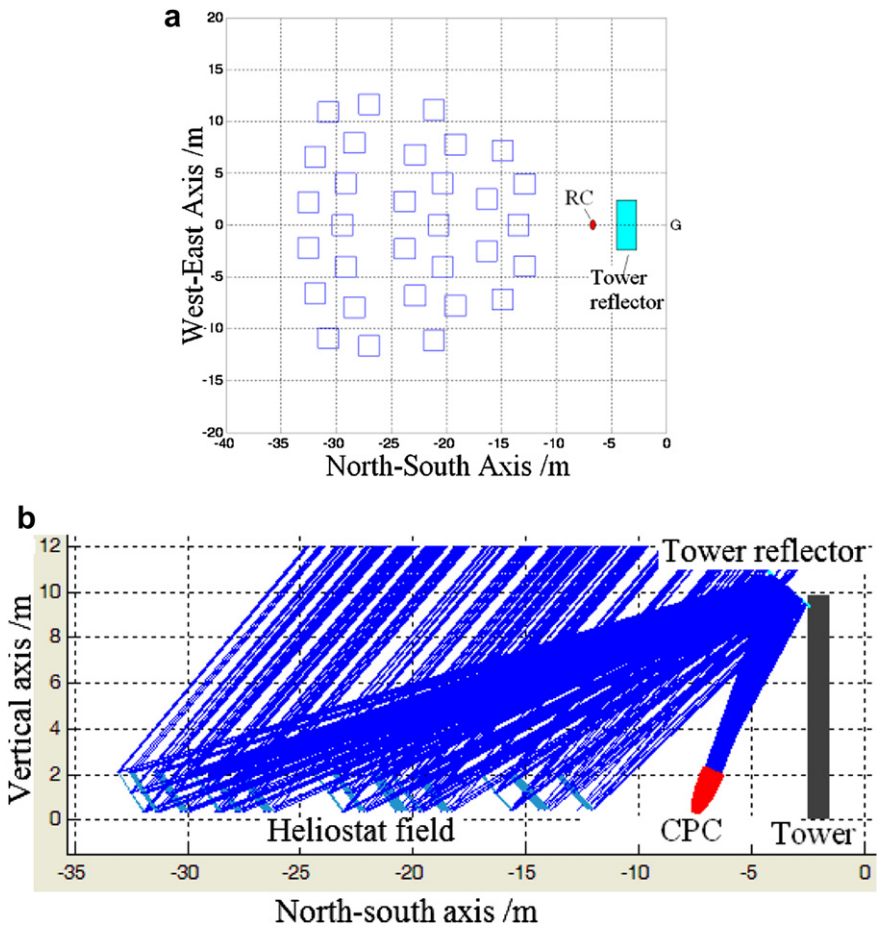

Fig. 4. Schematic of the beam-down solar concentrator, (a) The pattern of the field layout, (b) The three-dimensional case with traced rays. The dimensions shown are in meters.

Table 2
Parameters of the CPC concentrator.

Entrance aperture	1.036 m
Exit aperture $2a$	0.32 m
Overall length l	2.086 m
Focal length of the parabola f	0.209 m
Collecting angle θ_i	18°
Tilt angle δ_{RC}	10°
Reflectivity	0.95

In terms of the RC coordinate axes, the equations of the traced ray are written as follows,

$$\frac{x-x_A}{\cos\alpha_{rc}}=\frac{y-y_A}{\cos\beta_{rc}}=\frac{z}{\cos\gamma_{rc}} \tag{12}$$

By using Eq. (12), the coordinates of the intersection point between the traced ray and the entrance aperture of the RC can be calculated.

The CPC is usually selected as the RC. The CPC surface equation in the form $F(r, z) = 0$ is given as follows,

$$[r\cdot\cos\theta_i+\sin\theta_i\cdot(l-z)+a\cdot\cos\theta_i]^2+4\cdot f\cdot[r\cdot\sin\theta_i-\cos\theta_i\cdot(l-z)+a\cdot\sin\theta_i]-4\cdot f^2=0 \tag{13}$$

where θ_i is the collecting angle, a is the semidiameter of the exit aperture, l is the overall length of the CPC, and f is the focal length of a parabola. In terms of Cartesian coordinates, $r^2 = x^2 + y^2$, thus Eq. (13) can be written in the form $F(x, y, z) = 0$.

The direction cosine components ($\cos\alpha_{n2}$, $\cos\beta_{n2}$, $\cos\gamma_{n2}$) of the normal vector at a point of the CPC surface in the RC coordinate axes can be calculated as follows,

$$(\cos\alpha_{n2},\cos\beta_{n2},\cos\gamma_{n2})=(F_x,F_y,F_z)/\left(F_x^2+F_y^2+F_z^2\right)^{1/2} \tag{14}$$

where,

$$\begin{bmatrix}F_x\\F_y\\F_z\end{bmatrix}=\begin{bmatrix}2\cdot\cos\theta_i\cdot x\cdot\left\{\cos\theta_i+[\sin\theta_i\cdot(l-z)+a\cdot\cos\theta_i]/\sqrt{x^2+y^2}\right\}+4\cdot f\cdot\sin\theta_i\cdot x/\sqrt{x^2+y^2}\\2\cdot\cos\theta_i\cdot y\cdot\left\{\cos\theta_i+[\sin\theta_i\cdot(l-z)+a\cdot\cos\theta_i]/\sqrt{x^2+y^2}\right\}+4\cdot f\cdot\sin\theta_i\cdot y/\sqrt{x^2+y^2}\\-2\cdot\sin\theta_i\cdot\left[\cos\theta_i\cdot\sqrt{x^2+y^2}+\sin\theta_i\cdot\left(l-z\right)+a\cdot\cos\theta_i\right]+4\cdot f\cdot\cos\theta_i\end{bmatrix}.$$

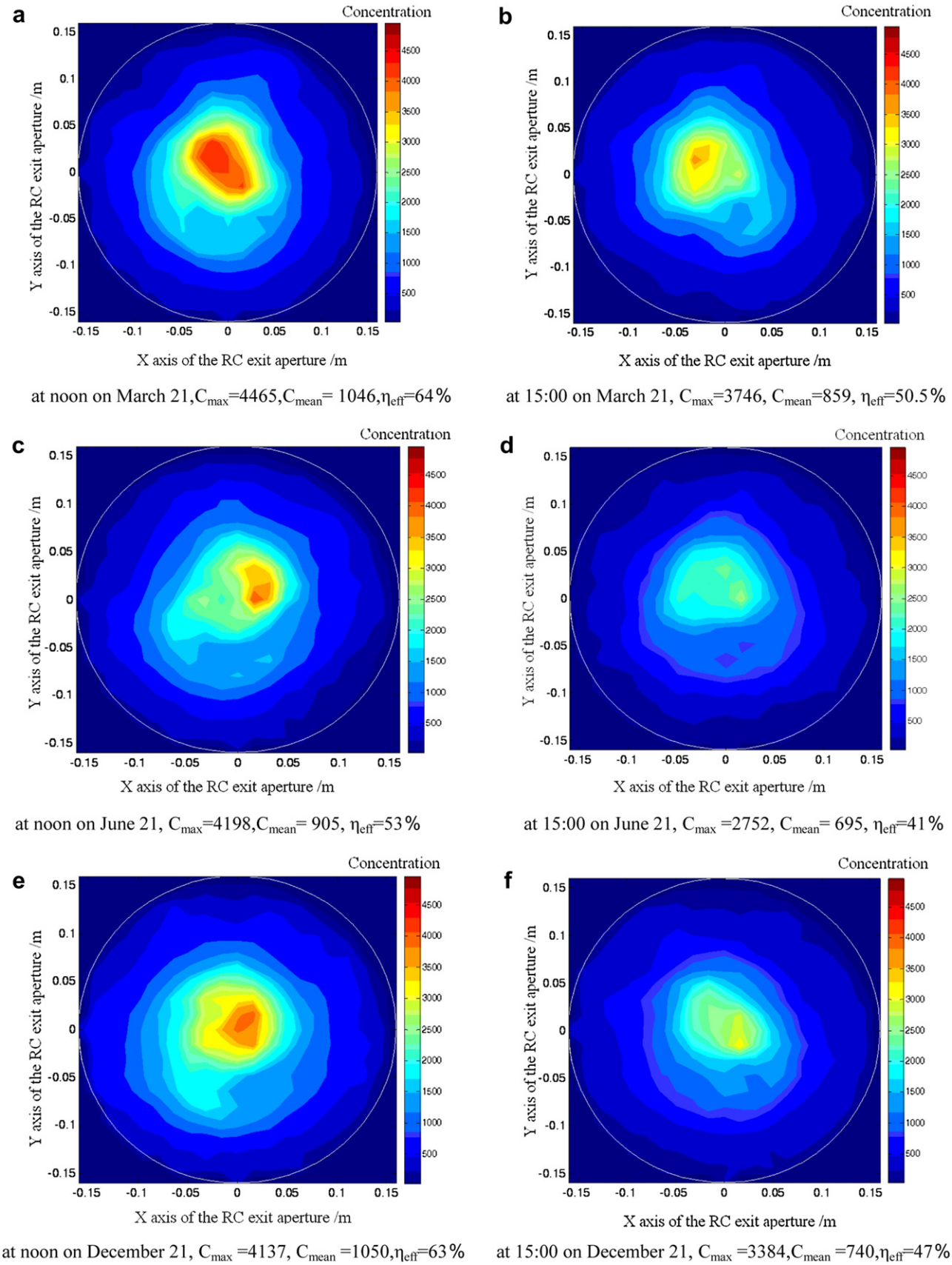

Fig. 5. The profile of the concentrated spot for the beam-down solar concentrator at different time, where the circle is the boundary of the exit aperture of CPC, C_{max} is the maximum concentration factor, C_{mean} is the mean concentration factor over the RC exit plane, η_{eff} is the optical efficiency, the concentration scale is 0–5000.

By inserting Eq. (12) into Eq. (13) and solving x, y and z, the coordinates (x_2, y_2, z_2) of the intersection point between the traced ray and the CPC surface can be obtained. By inserting (x_2, y_2, z_2) into Eq. (14), the normal vector at the intersection point of the CPC surface can be obtained.

According to the Snell law, the direction cosine components $(\cos\alpha_{r2}, \cos\beta_{r2}, \cos\gamma_{r2})$ of the reflection ray on the CPC surface in the RC coordinate axes are written as follows,

$$\begin{bmatrix} \cos\alpha_{r2} \\ \cos\beta_{r2} \\ \cos\gamma_{r2} \end{bmatrix} = \begin{bmatrix} 2\cdot\cos\theta_2\cdot\cos\alpha_{n2} - \cos\alpha_{rc} \\ 2\cdot\cos\theta_2\cdot\cos\beta_{n2} - \cos\beta_{rc} \\ 2\cdot\cos\theta_2\cdot\cos\gamma_{n2} - \cos\gamma_{rc} \end{bmatrix} \tag{15}$$

Where θ_2 is the reflection angle and the cosine of θ_2 can be written as,

$$\cos\theta_2 = \cos\alpha_{rc}\cdot\cos\alpha_{n2} + \cos\beta_{rc}\cdot\cos\beta_{n2} + \cos\gamma_{rc}\cdot\cos\gamma_{n2} \tag{16}$$

In terms of the RC coordinate axes, the equations of the reflection ray on the CPC surface can be written as follows,

$$\frac{x - x_2}{\cos\alpha_{r2}} = \frac{y - y_2}{\cos\beta_{r2}} = \frac{z - z_2}{\cos\gamma_{r2}} \tag{17}$$

If the reflection ray on the CPC surface intersects with the exit aperture plane, by inserting equation $z = -l$ into Eq. (17) and solving x, y and z, the coordinates of the intersection point can be derived as follows,

$$\begin{bmatrix} x_a \\ y_a \\ z_a \end{bmatrix} = \begin{bmatrix} (-l - z_2)\cdot\cos\alpha_{r2}/\cos\gamma_{r2} + x_2 \\ (-l - z_2)\cdot\cos\beta_{r2}/\cos\gamma_{r2} + y_2 \\ -l \end{bmatrix} \tag{18}$$

If the reflection ray on the CPC surface intersects with the CPC surface again, i.e., the traced ray are reflected more than once within the CPC, by inserting Eq. (17) into Eq. (13) and solving x, y and z, the coordinates (x_3, y_3, z_3) of the intersection point on the CPC surface can be obtained. By repeating the above calculations from Eq. (14) to Eq. (18), the coordinates of intersection points between all traced rays and the exit aperture plane of the CPC can be derived and the reflection times of the traced rays within the CPC can be counted finally.

3. The validation of the ray tracing equations

Based on the ray tracing equations, a new module for the simulation of the beam-down solar concentrator has been developed and incorporated into the code HFLD. To prove the correctness of the equations, the concentrated spots at the lower focal point of the tower reflector for a simple beam-down system are calculated at different time by both the modified code HFLD and the commercial software Zemax respectively. The calculated beam-down system consists of 3 heliostats and a hyperboloid tower reflector. The parameters of the heliostats and tower reflector are shown in Table 1.

The comparisons of the results are shown in Fig. 3. 13 × 13 beams have been considered in the comparison for each heliostat. The beams include edge beams, central beams, meridional beams and sagittal beams and so forth that are uniform distribution on the heliostat. It can be seen that the results coincide with each other basically. For the lack of information about Zemax in detail, the deviation of calculation results between HFLD and Zemax can be explained as follows: (1) the drawing algorithm between HFLD and Zemax is different; (2) the accuracy of the calculation is different. Considering above reasons, the calculation errors can be ignored. Therefore, the correctness of the ray tracing equations for the beam-down system is proved.

4. The simulation of the beam-down solar concentrator

By using the modified code HFLD, a beam-down solar concentrator consisting of 31 heliostats, a tower reflector and a CPC has been designed and simulated. The designed field layout is shown in Fig. 4.

A hyperboloid surface described by Eq. (2) is selected as the initial tower reflector surface. The surface and the tilt angle of the tower reflector are then further optimized by using the code HFLD. The parameters of the heliostats and tower reflector are shown in Table 1. The CPC is used for the re-concentration of the spot. The configuration and the tilt angle of the CPC are also optimized by using the code HFLD. The optimum parameters of the CPC are shown in Table 2.

HFLD assumes that the mirror surface errors and tracking errors have a Gaussian distribution, and the RMS (root mean square) of them equals to 1 mrad and 2.5 mrad respectively. In consideration of the sun shape, the incident beam relative to a point of the mirror can be considered as a flat top cone with a vertex angle of $\varepsilon = 9.3$ mrad. The reflection ratio of the mirrors is assumed to be 0.95. The profile of the concentrated spot and the optical efficiency for the beam-down solar concentrator at different time have been calculated by using the code HFLD and are shown in Fig. 5. The concentrated spot and the optical efficiency depend on the losses in the heliostat field and the multi-reflection losses in the RC. The losses in the heliostat field including the cosine loss, spillage, shading and blocking loss change with the sun position. Therefore, the concentrated spot and the optical efficiency change with the sun position as shown in Fig. 5.

5. Conclusions

The beam-down solar concentrator usually consists of a heliostat field, a tower reflector and a CPC. It is necessary to develop a special program for the design and simulation of the beam-down solar concentrator. In this paper, the ray tracing equations for the beam-down solar concentrator have been derived. Based on the equations, a new module for the simulation of the beam-down system has been developed and incorporated into the code HFLD. The validation of the modified code HFLD has been proved. By using the code HFLD, a small beam-down solar concentrator consisting of 31 heliostats, a tower reflector and a CPC has been designed. The concentrated spot and optical efficiency of the beam-down system at different time over a year have been calculated. According to the calculated concentration ratio and optical efficiency, using the DNI data, the concentrated power on the receiver plane can be obtained. It can be seen that the beam-down concentrator has a higher concentration ratio which meets the high-temperature solar applications. Therefore, the beam-down concentrator can be used in the solar thermal power plant or solar furnace instead of the solar tower system.

Acknowledgments

The authors acknowledge the financial support from the National Basic Research Program of China (Grant # 2010CB227101) and the National Natural Science Foundation of China (No.11174275).

References

[1] Stine WB, Geyer M. Power from the sun. Available from: http://www.powerfromthesun.net/book.htm; 2001.
[2] Rabl A. Tower reflector for solar power plants. Solar Energy 1976;18:269–71.
[3] Segal A, Epstein M. Comparative performances of 'tower-top' and 'tower reflector' central solar receivers. Solar Energy 1999;65:207–26.

[4] Segal A, Epstein M. The optics of the solar tower reflector. Solar Energy 2000; 69:229–41.
[5] Segal A, Epstein M. Optimized working temperatures of a solar central receiver. Solar Energy 2003;75:503–10.
[6] Segal A, Epstein M. Solar ground reformer. Solar Energy 2003;75:479–90.
[7] Kribus A, Zaibel R, Segal A. Extension of the Hermite expansion method for Cassegrainian solar central receiver systems. Solar Energy 1998;63:337–43.
[8] Hasuike H, Yoshizawa Y, Suzuki A, Tamaura Y. Study on design of molten salt solar receivers for beam-down solar concentrator. Solar Energy 2006;80: 1255–62.
[9] Wieckert C, Frommherz U, Kräupl S, Guillot E, Olalde G, Epstein M, et al. A 300 kW solar chemical pilot plant for the carbothermic production of Zinc. Transactions of the ASME 2007;129:190–6.
[10] Wei XD, Lu ZW, Lin Z, Zhang HX, Ni ZG. Optimization procedure for design of heliostat field layout of a 1MW solar tower thermal power plant. 684119. Proceeding of SPIE 2007;6841:1–10.
[11] Wei XD, Lu ZW, Yu WX, Wang ZF. A new code for the design and analysis of the heliostat field layout for power tower system. Solar Energy 2010;84: 685–90.
[12] Korsch D. Reflective optics. Elsevier Academic Press, ISBN 0124211704; 1991.